BJ www.biochemj.org

BJ Plant

Biochem. J. (2012) **443**, 49–56 (Printed in Great Britain) doi:10.1042/BJ20111308

online data

Structure–function studies of a plant tyrosyl-DNA phosphodiesterase provide novel insights into DNA repair mechanisms of *Arabidopsis thaliana*

Hoyeun KIM*[1], Sang Hyeon NA*[1], So-Young LEE*, Young-Min JEONG*, Hyun-Ju HWANG*, Jae Young HUR*, Sang-Hyun PARK*, Je-Chang WOO† and Sang-Gu KIM*[2]

*Department of Biological Sciences, Seoul National University, Seoul 151-742, Republic of Korea, and †Department of Biology, Mokpo National University, Jeonnam 534-729, Republic of Korea

TDP1 (tyrosyl-DNA phosphodiesterase 1), a member of the PLD (phospholipase D) superfamily, catalyses the hydrolysis of a phosphodiester bond between a tyrosine residue and the 3′-phosphate of DNA. We have previously identified and characterized the *AtTDP* gene in *Arabidopsis thaliana*, an orthologue of yeast and human *TDP1* genes. Sequence alignment of TDP1 orthologues revealed that AtTDP has both a conserved C-terminal TDP domain and, uniquely, an N-terminal SMAD/FHA (forkhead-associated) domain. To help understand the function of this novel enzyme, we analysed the substrate saturation kinetics of full-length AtTDP compared with a truncated AtTDP mutant lacking the N-terminal FHA domain. The recombinant AtTDP protein hydrolysed a single-stranded DNA substrate with K_m and k_{cat}/K_m values of 703 ± 137 nM and $(1.5 \pm 0.04) \times 10^9 M^{-1} \cdot min^{-1}$ respectively. The AtTDP-(Δ1–122) protein (TDP domain) showed kinetic parameters that were equivalent to those of the full-length AtTDP protein. A basic amino acid sequence (RKKVKP) within the AtTDP-(Δ123–605) protein (FHA domain) was necessary for nuclear localization of AtTDP. Analysis of active-site mutations showed that a histidine and a lysine residue in each of the HKD motifs were critical for enzyme activity. Vanadates, inhibitors of phosphoryl transfer reactions, inhibited AtTDP enzymatic activity and retarded the growth of an *Arabidopsis tdp* mutant. Finally, we showed that expression of the *AtTDP* gene could complement a yeast *tdp1*Δ*rad1*Δ mutant, rescuing the growth inhibitory effects of vanadate analogues and CPT (camptothecin). Taken together, the results of the present study demonstrate the structure-based function of AtTDP through which AtTDP can repair DNA strand breaks in plants.

Key words: *Arabidopsis*, enzyme kinetics, SMAD/forkhead-associated domain, tyrosyl-DNA phosphodiesterase 1 (TDP1), tyrosyl-DNA phosphodiesterase (TDP) domain, vanadate analogue.

INTRODUCTION

TDP1 (tyrosyl-DNA phosphodiesterase 1) specifically hydrolyses the phosphodiester bond between a tyrosine residue and the 3′-phosphate of DNA in the DNA–TOP1 (topoisomerase I) complex [1]. The tyrosine residue of TOP1 cleaves one strand of DNA and forms a 3′-phosphotyrosine intermediate, changing DNA topology by altering the linkage of the DNA strand [2]. *TDP1* was first identified in *Saccharomyces cerevisiae* [3], where its protein was shown to remove TOP1-linked DNA breaks [4]. Yeast *tdp1* mutant cells are hypersensitive to CPT (camptothecin), an anticancer drug that stabilizes the transient TOP1–DNA complex [3,4].

On the basis of sequence comparison, the TDP1 protein has been shown to belong to the PLD (phospholipase D) superfamily, which comprises proteins that are ubiquitous in bacteria, yeast, plants and mammals [5]. Members of the PLD superfamily catalyse the hydrolysis of a phosphodiester bond in glycerophospholipids, such as phosphatidylcholine, generating phosphatidic acid and free choline [6]. They contain an N-terminal region that varies in both size and amino acid identity. The function of this variable N-terminal region is unknown. Indeed, deletion of the N-terminal amino acids of human TDP1 was not found to affect enzyme activity *in vitro* [6]. A universal structure in the PLD superfamily is a repeated catalytic HKD motif [$HXK(X)_4D(X)_6GSXN$], which arose as a result of a gene duplication event [3,6]. These HKD motifs have highly conserved histidine (H) and lysine (K) residues [6–10]. Crystal structure analysis revealed that a histidine and a lysine residue in both HKD motifs are clustered together at the active centre of the enzymes [11].

A point mutation (H493R) in the human *TDP1* gene is physiologically important, as, in the homozygous state, it is responsible for SCAN1 (spinocerebellar ataxia with axonal neuropathy), an autosomal recessive neurodegenerative syndrome [12]. This recessive mutation reduces enzyme activity and, importantly, causes the accumulation of a TOP1–DNA complex lesion. *TDP1*-mutant SCAN1 cells are defective in the repair of DNA single-stranded breaks induced by CPT [13–15]. Moreover, human TDP1 was found to repair single-stranded DNA breaks caused by ionizing radiation [16]. TDP1 has DNA and RNA exonuclease activity and can hydrolyse various substrates blocking 3′-termini at strand breaks, including 3′-phosphoglycolates, 3′-phosphoamide and terminal abasic sites [9,17,18].

We have previously identified AtTDP, an orthologue of human TDP1 in *Arabidopsis* [19]. Unlike yeast and human TDP1 proteins, AtTDP consists of two domains: a SMAD/FHA (forkhead-associated) domain in the N-terminal region and a TDP domain in the C-terminal region. AtTDP, like other TDP1 orthologues, can remove the tyrosyl group from tyrosyl-DNA substrate *in vitro*. Moreover, AtTDP protein showed substrate specificity for single-stranded, blunted, tailed and nicked duplex DNA. The knockout *tdp* mutant exhibited a dwarf phenotype due to reduced cell numbers, which was caused by the accumulation of DNA damage and progressive cell death during *Arabidopsis* development [19].

Abbreviations used: CPT, camptothecin; DAPI, 4′,6-diamidino-2-phenylindole; FHA, forkhead-associated; GFP, green fluorescent protein; MS, Murashige and Skoog; PEG, poly(ethylene glycol); PLD, phospholipase D; RFP, red fluorescent protein; RT, reverse transcription; SCAN1, spinocerebellar ataxia with axonal neuropathy; smGFP, soluble-modified GFP; TDP1, tyrosyl-DNA phosphodiesterase 1; TFL2, terminal flower 2; TOP1, topoisomerase I.

[1] These authors contributed equally to the article.

[2] To whom correspondence should be addressed (email: kimsg@snu.ac.kr).

Until now, little was known about the enzymatic function of TDP1 in plants. In the present study, we describe the possible roles of the TDP and FHA domains of TDP in *Arabidopsis*. Specifically, we demonstrate both that the TDP domain alone is sufficient to hydrolyse a 3′-phosphate DNA–tyrosine complex, and that the FHA domain is necessary for targeting to the nucleus and contains a putative novel nuclear localization signal sequence (RKKVKP). Taken together, the results of the present study suggest that the distinctive structure of *Arabidopsis* TDP1 protein causes it to have a molecular function unlike that of its yeast and human orthologues.

EXPERIMENTAL

Production of recombinant AtTDP-(Δ1–122) (TDP domain) protein

The region of the *AtTDP* gene encoding the TDP domain was amplified from the leaves of 2-week-old plants by RT (reverse transcription)–PCR (TaKaRa). RT–PCR was performed using the specific primers 5′-AGAGGATCCATGGCTGAAGACGATGTAGAG-3′ and 5′-TTGAGCTCCTATCTTGGCCAGACTTGTCCA-3′. The TDP domain sequence was PCR-amplified, and the PCR products were cloned into the pGEM-T Easy vector (Promega), then subcloned into a pET30a (+) vector and transferred to *Escherichia coli* BL21(DE3) cells. Recombinant TDP domain protein expression was induced by 1 mM IPTG (isopropyl β-D-thiogalactopyranoside) at 28 °C and the protein was purified using His-Bind Resin and the His-Bind Kit (Novagen), according to the manufacturer's protocol. The purity of the enzyme was verified by SDS/PAGE (12 % gel).

Enzyme assays and kinetic determination

The ability of AtTDP and the TDP domain to function as phosphodiesterases and cleave a tyrosyl residue were examined as described previously [19]. The 18-Y (5′-TCCGTTGAAGCCTGCTTT-Tyr-3′) oligonucleotide, an artificial substrate, was used for all enzyme assays. AtTDP or the TDP domain protein was incubated with 18-Y substrate in an appropriate buffer [50 mM Tris/HCl (pH 8.0), 80 mM KCl, 2 mM EDTA, 1 mM dithiothreitol, 40 μg/ml BSA and 5 % glycerol] at 28 °C for 5 min. Reactions (20 μl) were stopped by the addition of 10 μl of formamide quenching buffer. All of the reaction solutions were subjected to electrophoresis on a 20 % acrylamide sequencing gel (acrylamide/bisacrylamide = 29:1) and stained by GelRed (Sigma) in TBE buffer (1×TBE = 45 mM Tris/borate and 1 mM EDTA) for 30 min. To determine the kinetic parameters of the AtTDP and TDP domain proteins, each protein was incubated with various concentrations of 18-Y substrate. The amount of substrate converted into the product, 3′-phosphate oligonucleotide, was measured by densitometry analysis of the gel image. Initial velocities were determined by plotting the amount of 3′-phosphate oligonucleotide as a function of time. All lines extrapolated to zero product at the start of the reaction, and at least three time points were used to determine the velocity. The concentrations of enzymes were determined using the Bradford protein assay [20]. The specific activity was determined as μmol of product formed/min per mg of enzyme. The kinetic parameters, K_m, k_{cat} and k_{cat}/K_m, were determined by the Michaelis–Menten equation $V = (V_{max}[S])/(K_m + [S])$ and Lineweaver–Burk plot $1/V = (K_m/V_{max} \cdot 1/[S]) + 1/V_{max}$ and $k_{cat} = V_{max}/[E_0]$.

Subcellular localization

The AtTDP-(Δ123–605) (FHA domain) and AtTDP-(Δ1–122) (TDP domain) GFP (green fluorescent protein)-fusion proteins were generated using the same methods as described previously for AtTDP [19], by amplifying from cDNA using FHA domain primers (5′-GGATCCATGTTAAAGGAAGACAATTCATCTC-3′/5′-CATGGATCCTCTAGAGTCCCCCGT-3′) and TDP domain primers (5′-TGGATCCAAGGAGATATACCAATG-3′/5′-GGA TCCATAGCTTGAAGAAATGGTGACCAG-3′) containing a BamHI site respectively, and subcloned into the smGFP (soluble-modified GFP) vector. Rosette leaves of wild-type plants grown for 2 weeks were used for the isolation and transformation of protoplasts. Plasmid DNA (10 μg) containing the FHA domain–GFP or TDP domain–GFP constructs were transfected into *Arabidopsis* mesophyll protoplasts using the PEG [poly(ethylene glycol)] method [21]. Protoplasts were then incubated in the dark at 24 °C for 24 h. Images were obtained using a confocal microscope (Radiance 2000/MP, Bio-Rad Laboratories).

For generation of a GFP-fusion construct containing the basic amino acid sequence from the FHA domain, a duplex oligonucleotide (5′-pGATCCATGAGAAAGAAAGTGAAACCTAG-3′/5′-pGATCCTAGGTTTCACTTTCTTTCTCATG-3′) was synthesized by Biomedic. The basic amino acid sequence was subcloned into pUC19 containing a 35S::smGFP construct, and transfected into the protoplasts of *Arabidopsis thaliana* by PEG-calcium transfection [22]. After incubation of transfected protoplasts at room temperature (22 °C) for 16 h, DAPI (4′,6-diamidino-2-phenylindole, 10 μg/ml) staining was used to visualize protoplast nuclei as a control. Images of smGFP-fusion protein expression in transfected protoplasts stained with DAPI were obtained using a fluorescence microscope (DE/Axio Imager A1, Carl Zeiss) and a multi-photon CLSM (confocal laser-scanning microscope; DE/LSM 510 NLO, Carl Zeiss). The excitation wavelength was 488 nm and emission was detected between 500 and 530 nm.

In vitro mutagenesis

Mutations of various residues in AtTDP to alanine (H236A, K238A, H466A and K468A) were produced by Mutagenex and confirmed by sequencing. The PCR-amplified products were treated with PNK (polynucleotide kinase) and DpnI, and then purified from an agarose gel. The purified PCR products were self-ligated and transformed. To generate each mutant plasmid, we amplified the whole vector using two mutagenic primers. The primer sequences used were as follows: H236A-F2, 5′-**gcT**TCGAAGGCTATATTTCTTG-3′; H236A-R2, 5′-GTGTGTCCCGAATGAAATAG-3′; K238A-F3, 5′-**gcG**GCTATATTTCTTGTCTATC-3′; K238A-R3, 5′-CGAATGGTGTGTCCCGAATG-3′; H466A-F, 5′-**gcT**ATAAAGACGTTCACACGTTAC-3′; H466A-R, 5′-TGGCATGGCACGACCGC-3′; K468A-F, 5′-**gcG**ACGTTCACACGTTACAACG-3′; and K468A-R, 5′-TATATGTGGCATGGCACG-3′. The mutant plasmids were introduced into *E. coli* BL21 (DE3) cells using the pET expression system (Novagen). The recombinant protein products were purified using His-Bind Resin and the His-Bind Kit (Novagen), according to the manufacturer's instructions.

Vanadate analogue treatment and measurement of total chlorophyll content in *Arabidopsis tdp* and wild-type plants

We evaluated the sensitivity of wild-type and *tdp* plants to vanadate analogues. All *Arabidopsis* plants used were ecotype Columbia. The loss-of-function AtTDP mutation was isolated from an *Arabidopsis* activation T-DNA (transferred DNA) tagging mutant pool as described by Lee et al. [19]. Homozygous *tdp* mutant and wild-type plants were germinated on plates

containing half-strength MS (Murashige and Skoog) medium, 1 % (w/v) sucrose and 0.7 % agar. Seedlings (5-day-old) were transferred on to MS plates supplemented with various concentrations of the vanadate analogues. Seedlings in vanadate-treated medium were allowed to grow for approximately 2 weeks. They were grown at 21 °C under constant light or 22 °C with a regime of 16 h of light/8 h of dark. The vanadate-treated wild-type and *tdp* mutant seedlings were freshly weighed and ground in 25 mM Hepes (pH 7.5) and 80 % acetone solution. The extracts of *Arabidopsis* seedlings were centrifuged and the supernatant was used in this experiment. The total chlorophyll content was measured as described by Porra [23]. Briefly, the absorbance of the supernatants at 646.6 nm and 663.6 nm was measured using a spectrophotometer (GE Healthcare), and chlorophyll content was calculated using the following equation: $\text{Chls}_{a+b} = 17.76A_{646.6} + 7.34A_{663.6}$.

Yeast strains and measurement of drug sensitivity

Yeast strains YW465 (*MATa*), YW812 (YW465 *tdp1Δ*::*kanMX4rad1Δ*::*HIS3*), YW463 (YW465 *rad1Δ*::*HIS3*) and YW625 (YW465 *tdp1Δ*::*URA3*) were used in the present study. Full-length AtTDP and the TDP domain sequence were subcloned into the p424 ADH vector (generating the p424 ADH–AtTDP and p424 ADH–TDP domain plasmids) [24]. To test sensitivity to CPT and vanadate analogues, yeast strains were grown at 30 °C in YPD [1 % (w/v) yeast extract/2 % (w/v) peptone/2 % (w/v) glucose] or selective medium containing 2 % (w/v) dextrose-tryptophan, with or without 20 μM CPT or 1 mM vanadate analogues. Plates were incubated at 30 °C for 2 days, and then photographed.

RESULTS

Substrate saturation kinetics of AtTDP protein

We previously determined that AtTDP catalyses the hydrolysis of the phosphodiester bonds between a tyrosine residue and the 3′-phosphate of DNA [19]. To further examine the kinetic parameters of the AtTDP protein, we carried out enzyme reactions with the synthesized single-stranded 18-Y oligonucleotide, which is an 18-mer containing a tyrosine residue at the 3′-terminus, as the substrate (Supplementary Figure S1 at http://www.BiochemJ.org/bj/443/bj4430049add.htm). The recombinant AtTDP has a molecular mass of 70 kDa. As shown in Figure 1 (inset), AtTDP protein efficiently hydrolysed the phosphodiester bond between tyrosine and the 3′-end of the DNA strand, and the amount of product formed was proportional to the assay time. We further examined enzyme activity using serial dilutions of 18-Y substrate. The Michaelis–Menten plot of AtTDP protein activity produced a typical hyperbolic curve (Supplementary Figure S2A at http://www.BiochemJ.org/bj/443/bj4430049add.htm). The V_{max} of AtTDP was 7.9 ± 0.5 μmol of product formed/min per mg of protein and the turnover number of the enzyme (k_{cat}) was 1077 ± 242 min^{-1} (Figure 2 and Table 1).

Substrate saturation kinetics of *Arabidopsis* AtTDP-(Δ1–122) (TDP domain) protein

AtTDP consists of a SMAD/FHA domain and a TDP domain [19]. The TDP domain is the most highly conserved domain of AtTDP, as in yeast and human TDP1, which is consistent with its role as a member of the PLD superfamily. To determine whether the TDP domain is responsible for the enzymatic activity of the protein, we generated a recombinant TDP domain polypeptide consisting of amino acids 123–605, using the pET expression system

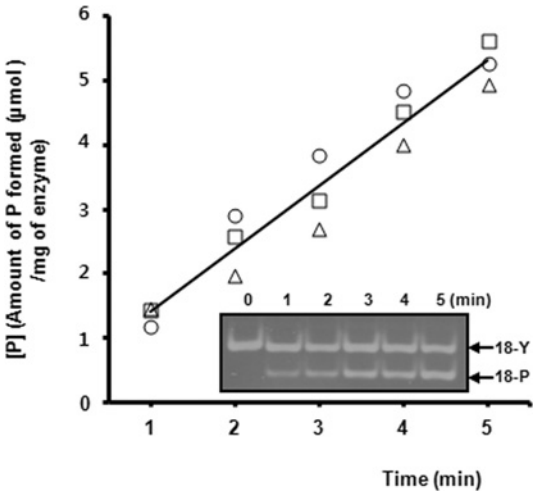

Figure 1 Time-dependence of AtTDP activity

The reaction was performed by incubating 0.1 ng of enzyme with 1.5 μM 18-Y substrate at 28 °C. The reaction velocity plot was generated by measuring the amount of 18-P product. The inset shows a gel image of a cleavage reaction used to calculate a reaction velocity. Reaction products before the addition of AtTDP protein (lane 1), and 1, 2, 3, 4 and 5 min after the addition of enzyme (lanes 2–6) are shown. All experiments were performed three times. Products were measured by densitometry after separation on a 20 % polyacrylamide gel.

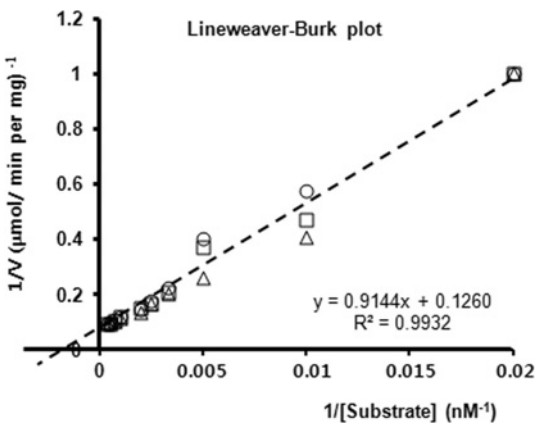

Figure 2 Determination of the kinetic parameters K_m and k_{cat} for AtTDP protein

Lineweaver–Burk plot of AtTDP activity. The reactions were performed by incubating 1 ng of enzyme and a variety of concentrations of 18-Y substrate at 28 °C. Reactions were terminated after 5 min by the addition of formamide quenching solution. All experiments were performed three times. Products were measured by densitometry after separation on a 20 % polyacrylamide gel.

(Novagen). The recombinant TDP domain protein has a molecular mass of 57 kDa. The TDP domain efficiently hydrolysed the phosphodiester bond between tyrosine and the 3′-end of DNA. The amount of product formed was proportional to the assay time (Figure 3). On the basis of the reciprocal Lineweaver–Burk plot (correlation coefficient $r^2 = 0.9989$, Figure 4), the recombinant TDP domain has a V_{max} of 8.0 ± 0.9 μmol of product formed/min per mg of enzyme and a k_{cat} of 950 ± 115 min^{-1} (Table 1 and Figure 4, and Supplementary Figure S2B).

The FHA domain basic amino acid sequence, RKKVKP, is a nuclear localization signal

AtTDP has a distinctive additional FHA domain in the N-terminal region, from amino acids 16 to 109. In sequence

Table 1 Summary of kinetic properties of recombinant AtTDP and TDP domain proteins

Values are means ± S.D. ($n = 3$)

Enzyme	K_m (nM)	k_{cat} (min^{-1})	k_{cat}/K_m ($M^{-1}\cdot min^{-1}$)
AtTDP	703 ± 137	1077 ± 242	$1.5 \times 10^9 \pm 0.04 \times 10^9$
TDP domain	770 ± 93	950 ± 115	$1.2 \times 10^9 \pm 0.02 \times 10^9$

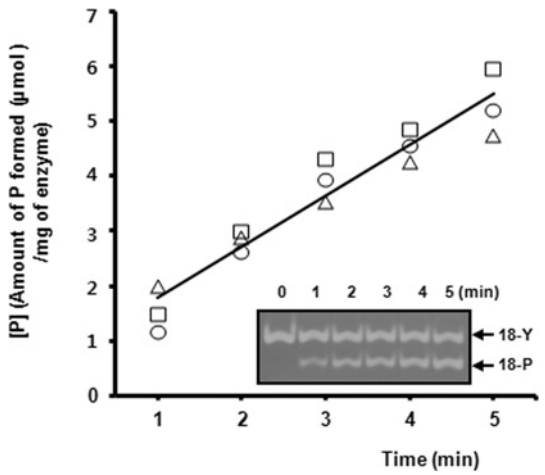

Figure 3 Time-dependence of AtTDP-(Δ1–122) (TDP domain) activity

The reaction was performed by incubating 0.1 ng of enzyme with 1.5 μM 18-Y substrate at 28 °C. The reaction velocity plot was generated by measuring the amount of 18-P product. The inset shows a gel image of a cleavage reaction used to calculate a reaction velocity. Reaction products before the addition of the TDP domain protein (lane 1), and 1, 2, 3, 4 and 5 min after the addition of enzyme (lanes 2–6) are shown. All experiments were performed three times. Products were measured by densitometry after separation on a 20 % polyacrylamide gel.

comparisons between *Arabidopsis* and yeast or human TDP1, the N-terminal region exhibited 15 and 25 % identity respectively (Supplementary Figure S3 at http://www.BiochemJ.org/bj/443/bj4430049add.htm). Among plants, TDP1 proteins showed approximately 35–45 % identity with *Arabidopsis* AtTDP (Supplementary Figure S4 at http://www.BiochemJ.org/bj/443/bj4430049add.htm). Among them, the *Medicago truncatula* Tdp1 proteins contained an FHA domain, in common with AtTDP, but its function has not been determined. To investigate the role of the FHA domain, we separated the FHA domain [AtTDP-(Δ123–605)] and the TDP domain [AtTDP-(Δ1–122)] and fused each to smGFP (Figures 5A and 5B). As a control, the *RFP* (red fluorescent protein) gene fused to *TFL2* (terminal flower 2) was expressed under the control of the CaMV (cauliflower mosaic virus) 35S promoter. The results show that the FHA domain–GFP fusion protein was targeted to the nucleus (Figures 5C–5E), whereas the TDP domain–GFP fusion protein was expressed in the cytosol (Figures 5F–5H). Thus we further examined whether a specific amino acid sequence within the FHA domain acts as a nuclear localization signal. We chose a short basic amino acid sequence, RKKVKP, from the FHA domain and performed *in vivo* targeting experiments using a construct composed of this basic sequence fused with smGFP (Figure 5I). The construct showed efficient nuclear localization (Figures 5J–5M). Specifically, more than 80 % of RKKVKP–GFP was localized to the nucleus (Supplementary Figure S5 at http://www.BiochemJ.org/bj/443/bj4430049add.htm).

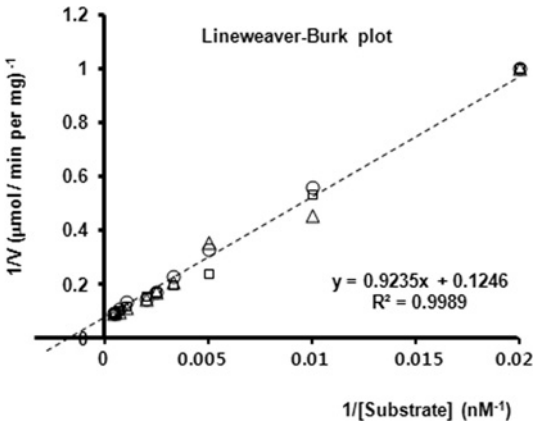

Figure 4 Determination of the kinetic parameters K_m and k_{cat} for AtTDP-(Δ1–122) (TDP domain) protein

Lineweaver–Burk plot of the TDP domain protein activity. The reactions were performed by incubating 1 ng of enzyme and a variety of concentrations of 18-Y substrate at 28 °C. Reactions were terminated after 5 min by the addition of formamide quenching solution. All experiments were performed three times. Products were measured by densitometry after separation on a 20 % polyacrylamide gel.

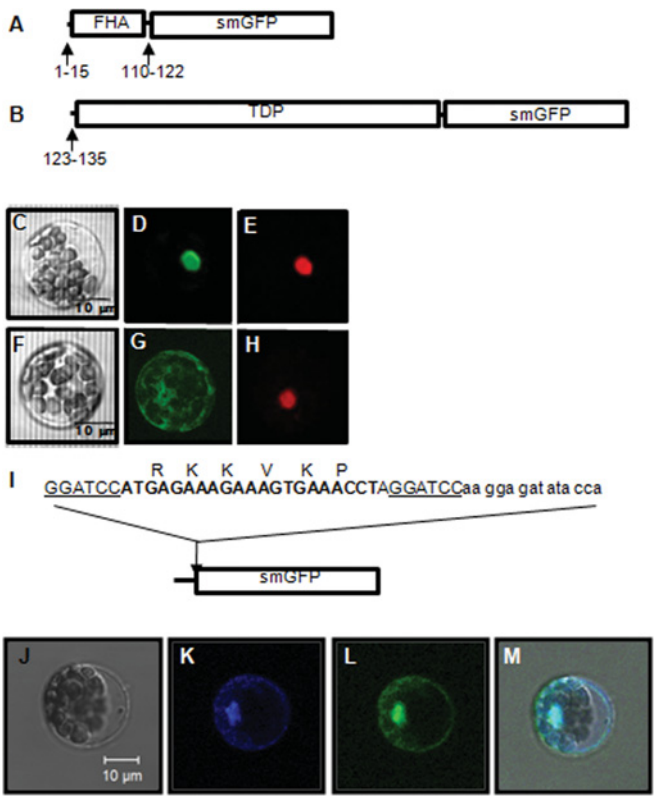

Figure 5 Subcellular localization of the isolated TDP and FHA domains from AtTDP

Schematic diagrams of the (**A**) FHA domain–smGFP and (**B**) TDP domain–smGFP constructs. (**C**) Light microscope image, (**D**) GFP fluorescence and (**E**) RFP fluorescence of a protoplast transfected with FHA domain–GFP and TFL2–RFP. TFL2–RFL expression indicates the nucleus. (**F**) Light microscope image, (**G**) GFP fluorescence and (**H**) RFP fluorescence of a protoplast transfected with TDP domain–GFP and TFL2–RFP. (**I**) The basic amino acid sequence within the FHA domain–smGFP construct. A transparent protoplast transfected with the basic amino acid sequence–GFP construct is shown (**J**) under a light microscope, (**K**) by DAPI fluorescence, (**L**) by GFP fluorescence and (**M**) with images from (**J**), (**K**) and (**L**) merged.

Table 2 The enzymatic activities of AtTDP proteins with mutated amino acid residues in the HKD motifs

Values are means ± S.D. ($n = 3$). ND, the H236A mutation completely suppressed the enzyme activity.

Enzyme/mutant	Specific activity (μmol of substrate converted into product/min per mg of enzyme)	Fold reduction
AtTDP	1.5 ± 0.5	1
H236A	ND	–
K238A	0.16 ± 0.001	9.4
H466A	0.015 ± 0.008	100
K468A	0.016 ± 0.001	94

Mutation of the most conserved amino acid residues in the HKD motifs drastically reduces the enzymatic activity of TDP protein

Being members of the PLD superfamily, TDP1 orthologues have highly conserved histidine and lysine residues in both of their C-terminal HKD motifs (Supplementary Figure S6A at http://www.BiochemJ.org/bj/443/bj4430049add.htm). Four conserved histidine and lysine residues (His^{263}, His^{493}, Lys^{265} and Lys^{495}) within the HKD motifs are necessary for the catalytic mechanism of human TDP1 [6]. To confirm whether the conserved amino acid residues of the HKD motifs in *Arabidopsis* also contribute to the active site, we generated several missense mutations of these residues (Table 2 and Supplementary Figure S6B). Mutation of His^{236} to an alanine (H236A) completely disrupted the enzymatic activity of AtTDP. As shown by the appearance of the product 18-P, mutation of Lys^{238} to an alanine (K238A) was approximately 10-fold less active than AtTDP (Table 2 and Supplementary Figure S7 at http://www.BiochemJ.org/bj/443/bj4430049add.htm). Mutation of His^{466} (H466A) or Lys^{468} (K468A) reduced enzymatic activities by ~100-fold respectively (Table 2 and Supplementary Figure S7).

Vanadate analogues inhibit AtTDP enzyme activity

Vanadate analogues (transition metal oxoanions) directly bind to tyrosine [25] and are known to be inhibitors of a variety of enzymes that are involved in phosphoryl transfer reactions. Their inhibitory effects may be based on their ability to mimic phosphates or act as transition stage analogues [26]. In addition to TDP1, some other members of the PLD superfamily are also inhibited by vanadate [27]. The human TDP1–vanadate complex structure has a trigonal bipyramidal geometry that mimics the transition state of hydrolysis of a phosphodiester bond [8].

To determine which vanadate analogues were more effective inhibitors of AtTDP activity, we assayed the enzyme activities of AtTDP and the TDP domain proteins in the presence of various vanadates. The enzymatic activities of AtTDP and the TDP domain proteins were completely inhibited by treatment with 20 and 40 mM sodium orthovanadate respectively. Furthermore, AtTDP and the TDP domain proteins were partially inhibited by treatment with sodium metavanadate and ammonium metavanadate (Figure 6 and Supplementary Figure S8 at http://www.BiochemJ.org/bj/443/bj4430049add.htm).

We further examined *in vivo* whether vanadate analogues affect the growth of wild-type or *tdp* mutant plants. The seedlings of wild-type and *tdp* mutant plants were grown in the presence of various concentrations of vanadate analogues. The *tdp* mutant plants were significantly hypersensitive to vanadate analogues (Figure 7). At a concentration of 0.05 mM, vanadate analogues caused severe growth defects in *AtTDP* loss-of-function mutant plants relative to wild-type (Figure 7).

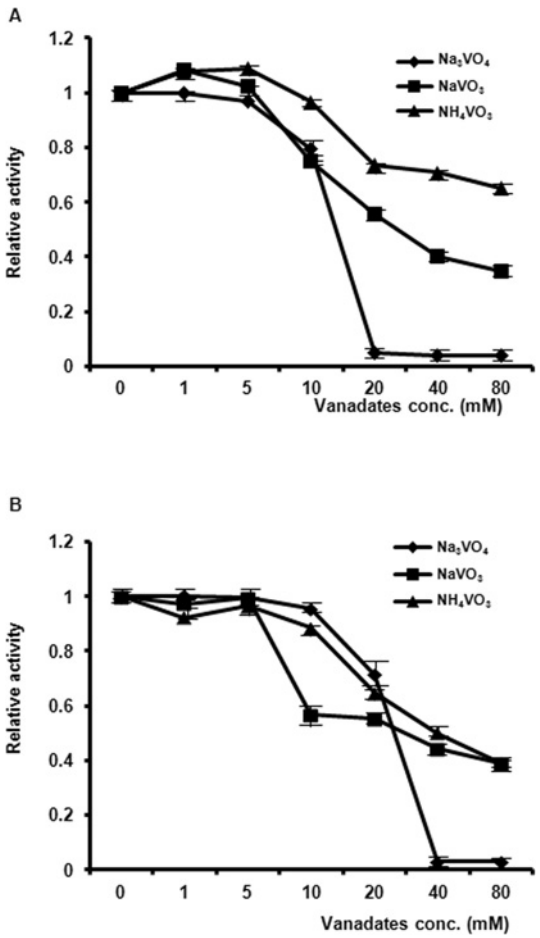

Figure 6 Inhibitory effects of vanadate analogues

(**A**) AtTDP protein and (**B**) TDP domain protein. Enzyme reactions were performed by incubating 0.1 ng of enzyme with 0.5 μM 18-Y substrate at 28 °C. A dilution series of the vanadate analogues was used. The reactions were terminated after 5 min by adding formamide quenching solution. The reaction velocity plots were generated by measuring the amount of 18-P products. Values are means ± S.D. (three independent replicates). Products were measured by densitometry after separation on a 20 % polyacrylamide gel. Na_3VO_4, sodium orthovanadate; $NaVO_3$, sodium metavanadate; NH_4VO_3, ammonium metavanadate.

Test for complementation of *tdp1*Δ*rad1*Δ mutant yeast by AtTDP and the TDP domain

The budding yeast (*Saccharomyces cerevisiae*) *tdp1*Δ*rad1*Δ strain exhibits a TOP1-dependent growth delay and shows significant sensitivity to CPT [28]. CPT stabilizes the TOP1–DNA complex and is an effective chemotherapeutic agent [25]. To test whether the yeast *tdp1*Δ*rad1*Δ strain could be complemented by the introduction of plant AtTDP, we examined the CPT and vanadate analogue sensitivity of *tdp1*Δ*rad1*Δ and of *tdp1*Δ*rad1*Δ strains expressing full-length AtTDP or the TDP domain. When the *tdp1*Δ*rad1*Δ strain was exposed to CPT, it showed a significant sensitivity, in contrast with wild-type, *tdp1*Δ, or *rad1*Δ strains (Supplementary Figure S9 at http://www.BiochemJ.org/bj/443/bj4430049add.htm). However, *tdp1*Δ*rad1*Δ expressing full-length AtTDP or the TDP domain did not show significant sensitivity to CPT (Figure 8, left-hand panel). None of the strains examined (*tdp1*Δ*rad1*Δ, *tdp1*Δ*rad1*Δ expressing full-length AtTDP or *tdp1*Δ*rad1*Δ expressing the TDP domain) were sensitive to vanadate analogues (Figure 8, upper panels). However, *tdp1*Δ*rad1*Δ treated with vanadate analogues

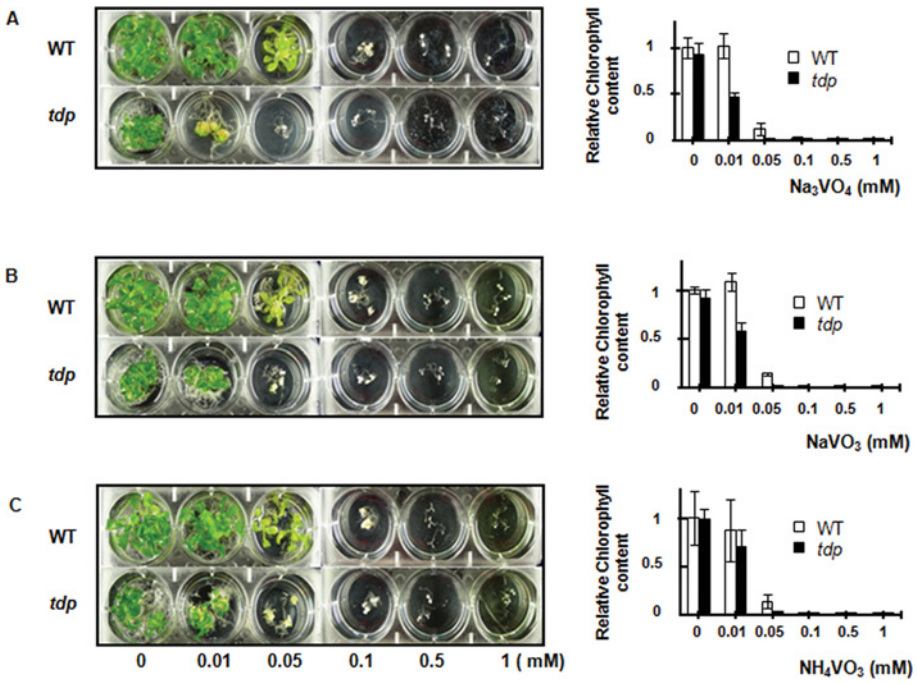

Figure 7 Inhibition of growth by vanadate analogues in wild-type and *tdp* mutant plants

Wild-type and *tdp* plants (20 days old) were treated with various concentrations of (**A**) sodium orthovanadate (Na_3VO_4) (left-hand panel), and the chlorophyll content of these plants was analysed (right-hand panel); (**B**) sodium metavanadate ($NaVO_3$) (left-hand panel), and the chlorophyll content of these plants was analysed (right-hand panel); and (**C**) ammonium metavanadate (NH_4VO_3) (left-hand panel), and the chlorophyll content of these plants was analysed (right-hand panel). Values are means ± S.D. (three independent replicates).

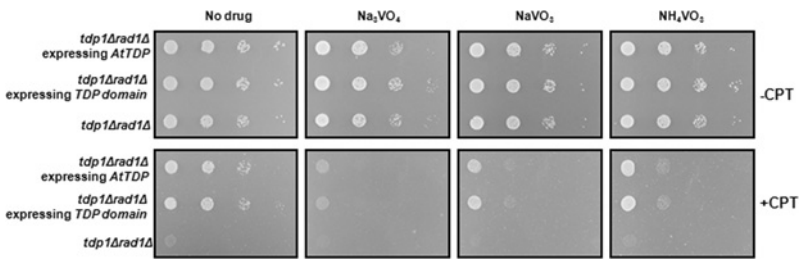

Figure 8 Complementation test in a *tdp1*Δ*rad1*Δ yeast strain

Serial dilutions of the *tdp1*Δ*rad1*Δ strain, *tdp1*Δ*rad1*Δ expressing full-length AtTDP or *tdp1*Δ*rad1*Δ expressing the TDP domain were spotted on to selective medium containing 2% (w/v) dextrose, with or without CPT and vanadate analogues.

displayed significant sensitivity to CPT, and expression of full-length AtTDP or the TDP domain partially rescued this sensitivity (Figure 8).

DISCUSSION

The TDP1 protein was originally found, in yeast cells, to be responsible for repair of the TOP1–DNA complex *in vivo*, catalysing the hydrolysis of topoisomerases from the 3′-end of DNA during double-strand break repair [3,4,29]. Similarly, in humans, TDP1 was found to participate in the repair of TOP1-induced lesions during single-strand break repair, and a recessive mutation of the *TDP1* gene is responsible for the hereditary disorder SCAN1 [12]. We previously identified and characterized a novel plant TDP1, the *Arabidopsis* TDP1 protein AtTDP. A loss-of-function mutation of AtTDP resulted in developmental defects and a dwarf phenotype in *Arabidopsis*. Recombinant AtTDP protein can hydrolyse the phosphodiester bond between a tyrosine residue and the 3′-terminus of single-stranded DNA, or blunted, tailed or nicked double-stranded DNA [19]. Recently, the expression profiles of the *MtTdp1α* and *MtTdp1β* genes in *Medicago truncatula* in response to oxidative stress have been reported [30].

On the basis of sequence alignments, TDP1 proteins have a highly conserved TDP domain at the C-terminus and poorly conserved sequence identity at the N-terminus. As members of the PLD superfamily, TDP1 orthologues, including AtTDP, have two highly conserved $HXK(X)_4D(X)_6GSXN$ sequences, known as HKD motifs, in the C-terminal region. To understand the structure-based function of the AtTDP protein, we created a TDP domain polypeptide through deletion of the N-terminal region, and compared the enzymatic kinetic parameters of the TDP domain with those of the full-length AtTDP protein. The turnover number of AtTDP and truncated TDP domain proteins for the single-stranded substrate seem to be identical as compared with those of human TDP1 ($\sim 1\times10^8$ $M^{-1}\cdot s^{-1}$) in the gel-based analysis of human TDP1 activity [31,32]. The results of

the present study demonstrate that the TDP domain is itself sufficient to confer the full phosphodiesterase activity of the AtTDP enzyme.

Sequence analysis of AtTDP showed it to contain a unique SMAD/FHA domain in the N-terminal region, unlike yeast and human TDP1s. SMAD/FHA domains are found as a component of forkhead transcription factor complexes and in various eukaryotic and prokaryotic signalling proteins involved in similar protein–protein interactions [33,34]. Generally, the FHA-domain-containing proteins in *Arabidopsis* show the conserved residues glycine, arginine, serine, histidine and asparagine within the FHA domain [35]. Even though the FHA domain of AtTDP only contains glycine, arginine, serine and histidine residues, it is still categorized as an FHA-domain-containing protein in TAIR (The *Arabidopsis* Information Resource, http://www.arabidopsis.org) and the Pfam-A matches (http://pfam.sanger.ac.uk).

In the case of AtTDP, although the FHA domain did not contain a known nuclear localization sequence, the FHA domain–GFP protein construct showed nuclear localization. We previously showed that full-length AtTDP protein is localized to the nucleus, whereas a TDP domain–GFP protein construct without the FHA domain is localized to the cytosol [19]. Therefore we focused on a possible nuclear-targeting amino acid sequence (RKKVKP) within the FHA domain of AtTDP, and generated a GFP construct to examine its nuclear localization. The results of the present study demonstrate that this basic amino acid sequence within the FHA domain possesses the ability to confer nuclear localization to AtTDP, which is consistent with its demonstrated enzyme activity. Human TDP1 contains two putative NLSs at residues 56–74 of the non-essential N-terminal region and residues 216–223 within its TDP domain, and must be efficiently localized and expressed in the nucleus for repair mechanisms [36,37].

In humans, a mutation in TDP1 was found to be responsible for the human genetic disorder SCAN1, an autosomal recessive disorder that arises as a result of a point mutation (H493R) in the second HKD motif [12]. Crystallographic studies of human TDP1 revealed that two conserved residues (histidine and lysine) in each HKD motif form an active site that is necessary for enzyme activity [7,8]. Various mutations (H263A, H493A, K265A or K495A) of the HKD motifs in human TDP1 reduce or abolish enzymatic activity [6,31]. To test whether plant TDP1 possesses the same active sites within the HKD motifs, we generated several point mutations in these motifs. The TDP1 reaction is a nucleophilic attack by His^{236} on the tyrosyl-DNA 3′ phosphate bond and this releases the DNA from this covalent intermediate [14]. Our results show that the H236A mutation (equivalent to H263A in human TDP1) within the first HKD motif completely obliterated the phosphodiesterase activity. Mutations of a lysine residue (Lys^{238}) in the first HKD motif, or the histidine (His^{466}) or lysine (Lys^{468}) residue of the second HKD motif also partially reduced the phosphodiesterase activity. Therefore we concluded that the catalytic mechanism of the plant enzyme is similar to that of other PLD family members.

In structural studies of human TDP1–vanadate complexes, the apparent trigonal bipyramidal geometry mimics the transition state of hydrolysis of a phosphodiester bond, with vanadate covalently bound to His^{263} [7,8]. Vanadates can also inhibit the enzyme activity of human TDP1 through a phosphate-mimicking function [38]. Using biochemical assays, we found that the enzyme activities of AtTDP and the TDP domain protein were completely or partially inhibited by sodium orthovanadate, sodium metavanadate and ammonium metavanadate. In addition, *Arabidopsis tdp* mutant plants were highly sensitive to very low concentrations of sodium orthovanadate and sodium metavanadate in *in vivo* experiments. These results may be explained by the possibility that somehow *tdp* mutant plants have plasma membranes that are more permeable to vanadates and/or have an increased affinity of membrane 'vanadate transporter proteins' for vanadates. However, future studies are needed determine the biochemical basis for this interesting observation.

Moreover, we assessed the *in vivo* ability of AtTDP and the TDP domain to rescue the sensitivity of a budding yeast *tdp1*Δ*rad1*Δ strain to CPT and vanadate analogues, since the treatment of both compounds should be explained by the synergy effect in complementation. CPT is an antitumour agent that acts as a topoisomerase inhibitor by binding to the covalent TOPI–DNA complex and preventing the DNA religation step [3]. The finding that full-length AtTDP or the TDP domain can rescue the sensitivity of a *tdp1*Δ*rad1*Δ strain to CPT and vanadate analogues suggests a role for AtTDP in the repair of damage induced by CPT and vanadate analogues.

In conclusion, the TDP domain alone is sufficient for enzyme activity, and the FHA domain of *Arabidopsis thaliana* TDP1 is necessary for its nuclear localization. A basic amino acid sequence within the FHA domain is a novel nuclear localization signal. Furthermore, inhibitor analysis increases our understanding of the dynamics of structure-based enzyme inhibition in plants.

AUTHOR CONTRIBUTION

Hoyeun Kim and Sang-Gu Kim designed the experiments and wrote the paper. Hoyeun Kim, Je-Chang Woo and Sang-Gu Kim analysed and interpreted the data. Hoyeun Kim, Sang Hyeon Na, Young-Min Jeong, So-Young Lee, Hyun-Ju Hwang and Jae Young Hur carried out the experiments. Sang-Hyun Park optimized the yeast experiments.

ACKNOWLEDGEMENTS

We thank Professor Donald J. Armstrong (Oregon State University, Corvallis, OR, U.S.A.) for his critical review of this paper prior to submission, Professor Thomas E. Wilson (University of Michigan Medical School, Ann Arbor, MI, U.S.A.) for providing yeast strains and Won-Ki Huh (Seoul National University, Seoul, Korea) for providing the p424 ADH vector.

FUNDING

This work was supported by a Korea Research Foundation Grant funded by the Korean Government (MOEHRD) [grant numbers KRF-2007-314-C00275, KRF-2008-313-C00841]; and the Basic Science Research Program through the National Research Foundation of Korea (NRF) funded by the Ministry of Education, Science and Technology [grant number 2011-0024730].

REFERENCES

1 Yang, S. W., Burgin, Jr, A. B., Huizenga, B. N., Robertson, C. A., Yao, K. C. and Nash, H. A. (1996) A eukaryotic enzyme that can disjoin dead-end covalent complexes between DNA and type I topoisomerases. Proc. Natl. Acad. Sci. U.S.A. **93**, 11534–11539
2 Wang, J. C. (2002) Cellular roles of DNA topoisomerases: a molecular perspective. Nat. Rev. Mol. Cell Biol. **3**, 430–440
3 Pouliot, J. J., Yao, K. C., Robertson, C. A. and Nash, H. A. (1999) Yeast gene for a Tyr-DNA phosphodiesterase that repairs topoisomerase I complexes. Science **286**, 552–555
4 Pouliot, J. J., Robertson, C. A. and Nash, H. A. (2001) Pathways for repair of topoisomerase I covalent complexes in *Saccharomyces cerevisiae*. Genes Cells **6**, 677–687
5 Ponting, C. P. and Kerr, I. D. (1996) A novel family of phospholipase D homologues that includes phospholipid synthases and putative endonucleases: identification of duplicated repeats and potential active site residues. Prot. Sci. **5**, 914–922
6 Interthal, H., Pouliot, J. J. and Champoux, J. J. (2001) The tyrosyl-DNA phosphodiesterase Tdp1 is a member of the phospholipase D superfamily. Proc. Natl. Acad. Sci. U.S.A. **98**, 12009–12014
7 Davies, D. R., Interthal, H., Champoux, J. J. and Hol, W. G. (2003) Crystal structure of a transition state mimic for Tdp1 assembled from vanadate, DNA, and a topoisomerase I-derived peptide. Chem. Biol. **10**, 139–147

8 Davies, D. R., Interthal, H., Champoux, J. J. and Hol, W. G. (2002) Insights into substrate binding and catalytic mechanism of human tyrosyl-DNA phosphodiesterase (Tdp1) from vanadate and tungstate-inhibited structures. J. Mol. Biol. **324**, 917–932
9 Interthal, H., Chen, H. J. and Champoux, J. J. (2005) Human Tdp1 cleaves a broad spectrum of substrates, including phosphoamide linkages. J. Biol. Chem. **280**, 36518–36528
10 Davies, D. R., Interthal, H., Champoux, J. J. and Hol, W. G. (2002) The crystal structure of human tyrosyl-DNA phosphodiesterase, Tdp1. Structure **10**, 237–248
11 Leiros, I., Secundo, F., Zambonelli, C., Servi, S. and Hough, E. (2000) The first crystal structure of a phospholipase D. Structure **8**, 655–667
12 Takashima, H., Boerkoel, C. F., John, J., Saifi, G. M., Salih, M. A., Armstrong, D., Mao, Y., Quiocho, F. A., Roa, B. B., Nakagawa, M. et al. (2002) Mutation of TDP1, encoding a topoisomerase I-dependent DNA damage repair enzyme, in spinocerebellar ataxia with axonal neuropathy. Nat. Genet. **32**, 267–272
13 Miao, Z. H., Agama, K., Sordet, O., Povirk, L., Kohn, K. W. and Pommier, Y. (2006) Hereditary ataxia SCAN1 cells are defective for the repair of transcription-dependent topoisomerase I cleavage complexes. DNA Repair **5**, 1489–1494
14 Interthal, H., Chen, H. J., Kehl-Fie, T. E., Zotzmann, J., Leppard, J. B. and Champoux, J. J. (2005) SCAN1 mutant Tdp1 accumulates the enzyme-DNA intermediate and causes camptothecin hypersensitivity. EMBO J. **24**, 2224–2233
15 El-Khamisy, S. F., Saifi, G. M., Weinfeld, M., Johansson, F., Helleday, T., Lupski, J. R. and Caldecott, K. W. (2005) Defective DNA single-strand break repair in spinocerebellar ataxia with axonal neuropathy-1. Nature **434**, 108–113
16 El-Khamisy, S. F., Hartsuiker, E. and Caldecott, K. W. (2007) TDP1 facilitates repair of ionizing radiation-induced DNA single-strand breaks. DNA Repair **6**, 1485–1495
17 Zhou, T., Lee, J. W., Tatavarthi, H., Lupski, J. R., Valerie, K. and Povirk, L. F. (2005) Deficiency in 3′-phosphoglycolate processing in human cells with a hereditary mutation in tyrosyl-DNA phosphodiesterase (TDP1). Nucleic Acids Res. **33**, 289–297
18 Inamdar, K. V., Pouliot, J. J., Zhou, T., Lees-Miller, S. P., Rasouli-Nia, A. and Povirk, L. F. (2002) Conversion of phosphoglycolate to phosphate termini on 3′ overhangs of DNA double strand breaks by the human tyrosyl-DNA phosphodiesterase hTdp1. J. Biol. Chem. **277**, 27162–27168
19 Lee, S. Y., Kim, H., Hwang, H. J., Jeong, Y. M., Na, S. H., Woo, J. C. and Kim, S. G. (2010) Identification of tyrosyl-DNA phosphodiesterase as a novel DNA damage repair enzyme in *Arabidopsis*. Plant Physiol. **154**, 1460–1469
20 Bradford, M. M. (1976) A rapid and sensitive method for the quantitation of microgram quantities of protein utilizing the principle of protein-dye binding. Anal. Biochem. **72**, 248–254
21 Dix, J. A., Verkman, A. S., Solomon, A. K. and Cantley, L. C. (1979) Human erythrocyte anion exchange site characterised using a fluorescent probe. Nature **282**, 520–522
22 Yoo, S. D., Cho, Y. H. and Sheen, J. (2007) *Arabidopsis* mesophyll protoplasts: a versatile cell system for transient gene expression analysis. Nat. Protoc. **2**, 1565–1572
23 Porra, R. J. (2002) The chequered history of the development and use of simultaneous equations for the accurate determination of chlorophylls a and b. Photosynth. Res. **73**, 149–156
24 Mumberg, D., Muller, R. and Funk, M. (1995) Yeast vectors for the controlled expression of heterologous proteins in different genetic backgrounds. Gene **156**, 119–122
25 Pommier, Y. (2006) Topoisomerase I inhibitors: camptothecins and beyond. Nat. Rev. Cancer **6**, 789–802
26 Zhang, M., Zhou, M., Van Etten, R. L. and Stauffacher, C. V. (1997) Crystal structure of bovine low molecular weight phosphotyrosyl phosphatase complexed with the transition state analog vanadate. Biochemistry **36**, 15–23
27 Li, L. and Fleming, N. (1999) Aluminum fluoride inhibition of cabbage phospholipase D by a phosphate-mimicking mechanism. FEBS Lett. **461**, 1–5
28 Vance, J. R. and Wilson, T. E. (2001) Repair of DNA strand breaks by the overlapping functions of lesion-specific and non-lesion-specific DNA 3′ phosphatases. Mol. Cell. Biol. **21**, 7191–7198
29 Vance, J. R. and Wilson, T. E. (2002) Yeast Tdp1 and Rad1-Rad10 function as redundant pathways for repairing Top1 replicative damage. Proc. Natl. Acad. Sci. U.S.A. **99**, 13669–13674
30 Macovei, A., Balestrazzi, A., Confalonieri, M. and Carbonera, D. (2010) The tyrosyl-DNA phosphodiesterase gene family in *Medicago truncatula* Gaertn.: bioinformatic investigation and expression profiles in response to copper- and PEG-mediated stress. Planta **232**, 393–407
31 Raymond, A. C., Rideout, M. C., Staker, B., Hjerrild, K. and Burgin, Jr, A. B. (2004) Analysis of human tyrosyl-DNA phosphodiesterase I catalytic residues. J. Mol. Biol. **338**, 895–906
32 Raymond, A. C., Staker, B. L. and Burgin, Jr, A. B. (2005) Substrate specificity of tyrosyl-DNA phosphodiesterase I (Tdp1). J. Biol. Chem. **280**, 22029–22035
33 Durocher, D. and Jackson, S. P. (2002) The FHA domain. FEBS Lett. **513**, 58–66
34 Hofmann, K. and Bucher, P. (1995) The FHA domain: a putative nuclear signalling domain found in protein kinases and transcription factors. Trends Biochem. Sci. **20**, 347–349
35 Chevalier, D., Morris, E. R. and Walker, J. C. (2009) 14-3-3 and FHA domains mediate phosphoprotein interactions. Annu. Rev. Plant Biol. **60**, 67–91
36 Barthelmes, H. U., Habermeyer, M., Christensen, M. O., Mielke, C., Interthal, H., Pouliot, J. J., Boege, F. and Marko, D. (2004) TDP1 overexpression in human cells counteracts DNA damage mediated by topoisomerases I and II. J. Biol. Chem. **279**, 55618–55625
37 Dexheimer, T. S., Antony, S., Marchand, C. and Pommier, Y. (2008) Tyrosyl-DNA phosphodiesterase as a target for anticancer therapy. Anticancer Agents Med. Chem. **8**, 381–389
38 Liao, Z., Thibaut, L., Jobson, A. and Pommier, Y. (2006) Inhibition of human tyrosyl-DNA phosphodiesterase by aminoglycoside antibiotics and ribosome inhibitors. Mol. Pharmacol. **70**, 366–372

Received 20 July 2011/21 December 2011; accepted 3 January 2012
Published as BJ Immediate Publication 3 January 2012, doi:10.1042/BJ20111308

Biochem. J. (2012) **443**, 49–56 (Printed in Great Britain) doi:10.1042/BJ20111308

online data

SUPPLEMENTARY ONLINE DATA

Structure–function studies of a plant tyrosyl-DNA phosphodiesterase provide novel insights into DNA repair mechanisms of *Arabidopsis thaliana*

Hoyeun KIM*[1], Sang Hyeon NA*[1], So-Young LEE*, Young-Min JEONG*, Hyun-Ju HWANG*, Jae Young HUR*, Sang-Hyun PARK*, Je-Chang WOO† and Sang-Gu KIM*[2]

*Department of Biological Sciences, Seoul National University, Seoul 151-742, Republic of Korea, and †Department of Biology, Mokpo National University, Jeonnam 534-729, Republic of Korea

Figure S1 Schematic diagram showing the reaction mechanism of AtTDP

AtTDP hydrolyses the tyrosine residue from the artificial synthesized single-strand 18-Y substrate containing a tyrosine residue.

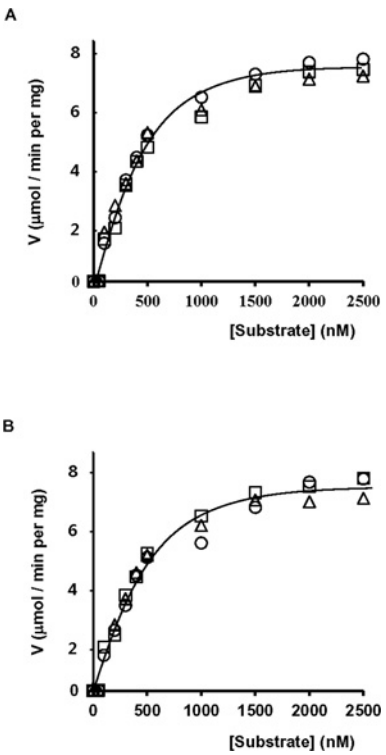

Figure S2 Michaelis–Menten plots of AtTDP and TDP domain activities

The saturation curves of AtTDP protein (**A**) and TDP domain protein (**B**). Enzyme reactions were performed by incubating 1 ng of enzyme and a variety of concentrations of 18-Y substrate at 28 °C. The reaction was stopped after 5 min by the addition of formamide quench solution. All experiments were performed three times. Products were measured by densitometry after separation on a 20 % polyacrylamide gel.

[1] These authors contributed equally to the article.
[2] To whom correspondence should be addressed (email: kimsg@snu.ac.kr).

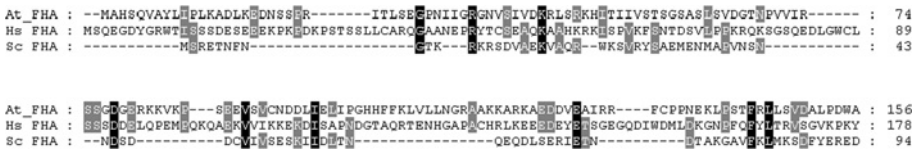

Figure S3 Alignments of the N-terminal region of Tdp1 proteins of yeast, human and *Arabidopsis*

Sequence alignment was analysed by the program ClustalW. Abbreviations and accession numbers are as follows: Sc (*Saccharomyces cerevisiae*, NCBI RefSeq accession number NP_009782), Hs (*Homo sapiens*, NCBI RefSeq accession number NP_060789) and At (*Arabidopsis thaliana*, NCBI RefSeq accession number NP_197021). Amino acid sequence identity (%) between AtTDP and hTdp1 was 25 %. The identity between AtTDP and yeast Tdp1 was 15 %. Black boxes indicated single fully conserved residues and grey boxes indicate conservation of weak groups.

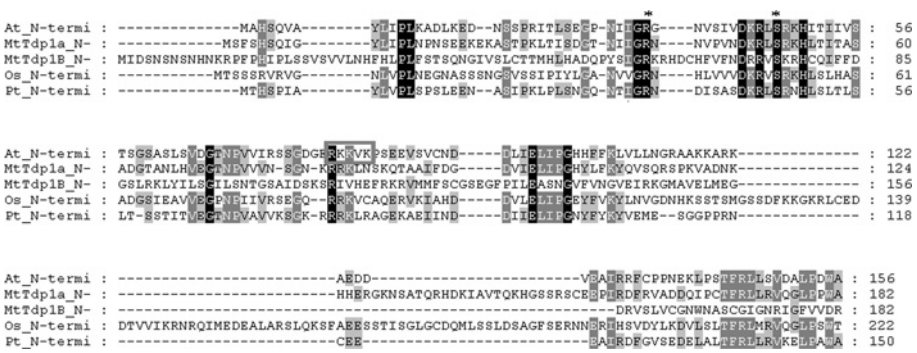

Figure S4 Alignments of the N-terminal region of plant Tdp1 proteins

Sequence alignment was analysed by the program ClustalW. Abbreviations and accession numbers are as follows: At (*Arabidopsis thaliana*, FHA domain, NCBI RefSeq accession number NP_197021), MtTdp1α (*Medicago truncatula*, FHA domain, GenBank® accession number ABE78603.1), MtTdp1β (*Medicago truncatula*, FHA domain, HIRAN domain, GenBank® accession number ABE85647.1), Os (*Oryza sativa*, FHA domain, NCBI RefSeq accession number NP_001059844) and Pt (*Populus trichocarpa*, FHA domain, GenBank® accession number EEE86125.1). Amino acid sequence identity (%) between AtTDP is follows: Mt, 42 %; Os, 35 %; and Pt, 45 %. Black boxes indicate single fully conserved residues and grey boxes indicate conservation of weak groups. Asterisks indicate the core FHA homology (arginine and serine). The AtTDP domain did not contain asparagine residues for the interaction with the FHA-domain-binding proteins.

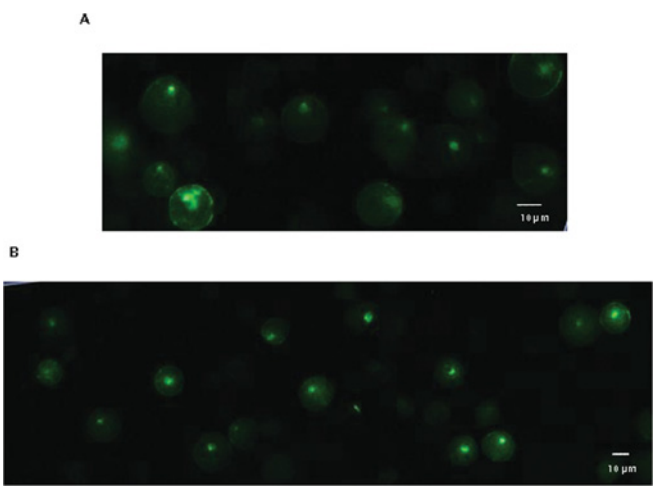

Figure S5 Subcellular localization of the basic amino acid sequence RKKVKP within the FHA domain

(**A**) and (**B**) Subcellular localization. Protoplasts expressing the RKKVKP–smGFP driven by the constitutive 35S enhancer were shown under fluorescence microscopy ($\times$100; DE/Axio Imager A1, Carl Zeiss). More than 80 % of the RKKVKP–GFP construct was successfully localized in the nucleus. The percentage of smGFP signalling protoplast/total protoplast in the slide glasses excluded the burst or wrinkled protoplasts.

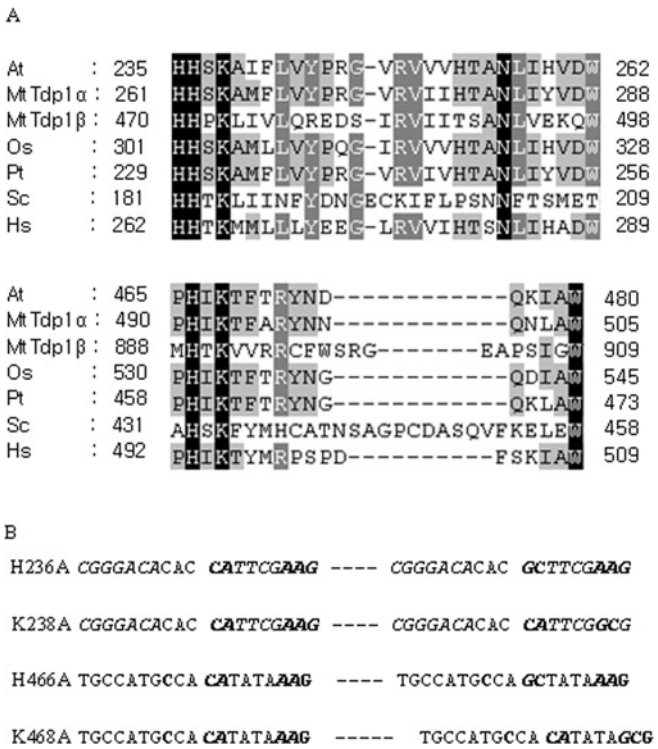

Figure S6 Sequence alignment of the HKD motifs in Tdp1 proteins and point mutations of the active-site residue of HKD motifs

(**A**) Sequence alignment of the HKD motifs in Tdp1 proteins were analysed by the program ClustalW. Abbreviations and accession numbers are as follows: At (*Arabidopsis thaliana*, NCBI RefSeq accession number NP_197021), MtTdp1α (*Medicago truncatula*, FHA domain, GenBank® accession number ABE78603.1), MtTdp1β (*Medicago truncatula*, FHA domain, HIRAN domain, GenBank® accession number ABE85647.1), Os (*Oryza sativa*, NCBI RefSeq accession number NP_001059844), Pt (*Populus trichocarpa*, GenBank® accession number EEE86125.1), Sc (*Saccharomyces cerevisiae*, NCBI RefSeq accession number NP_009782), Hs (*Homo sapiens*, NCBI RefSeq accession number NP_060789). Black boxes indicate single fully conserved residues and grey boxes indicate conservation of weak groups. (**B**) Point mutations of the active-site residue of HKD motifs in AtTDP protein.

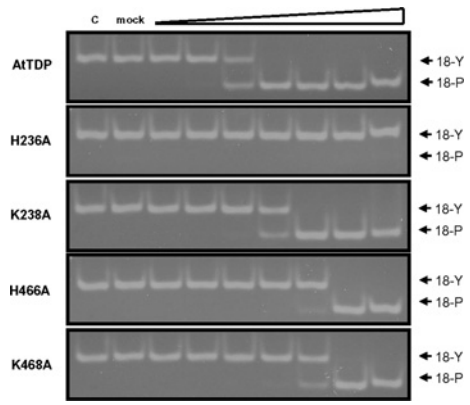

Figure S7 Enzymatic activity analyses of AtTDP proteins with mutated amino acid residues in the HKD motifs

The activities of full-length AtTDP protein and four mutated proteins were determined with single-stranded substrate. The conserved His^{236}, Lys^{238}, His^{466} and Lys^{468} residues of both HKD motifs were mutated. Mock sample was the analogously prepared protein fraction derived from IPTG-induced BL21(DE3) cells containing pET30a(+) plasmid. The mock-purified preparations were tested at the highest concentration. Enzyme reactions were performed by incubating 0.5 μM 18-Y substrate and 10-fold serial dilutions of enzyme (0.01–10000 ng) at 28°C. The reaction was stopped after 5 min with the addition of formamide quench solution. All experiments were performed three times. Products were measured by densitometry after separation on a 20% polyacrylamide gel.

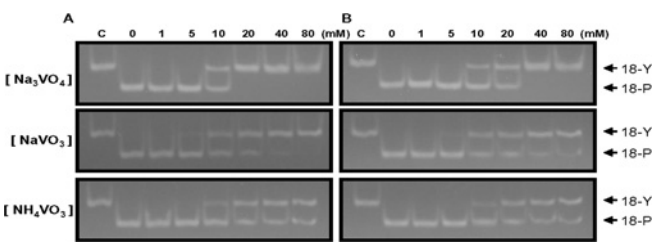

Figure S8 Inhibitory effects by vanadate analogues

(**A**) AtTDP protein or (**B**) TDP domain protein. Enzyme reactions were performed by incubating 1 ng of enzyme and 0.5 μM 18-Y substrate at 28°C. A dilution curve of vanadate analogue concentrations was used. The reaction was stopped after 5 min by adding formamide quench solution. The reaction velocity plots were calculated by measuring the amount of 18-P product. All experiments were performed three times. Products were measured by densitometry after separation on a 20% polyacrylamide gel. Na_3VO_4, sodium orthovanadate; $NaVO_3$, sodium metavanadate; NH_4VO_3, ammonium metavanadate.

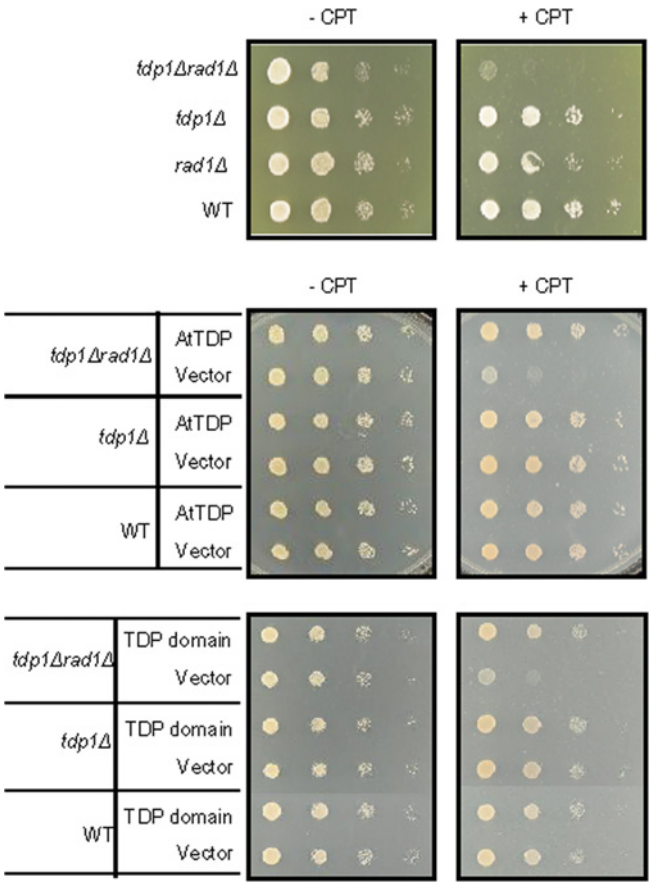

Figure S9 The complementation test in the *tdp1*Δ*rad1*Δ strain

Serial dilutions of *tdp1*Δ*rad1*Δ, *tdp1*Δ, *rad1*Δ and wild-type strains were spotted on to a YPD plate with or without CPT. The *tdp1*Δ *rad1*Δ, *tdp1*Δ and wild-type stains transformed with p424 ADH–AtTDP, p424 ADH–TDP domain and p424 ADH vector were spotted on to selective medium containing 2 % (w/v) dextrose plates with or without CPT.

Received 20 July 2011/21 December 2011; accepted 3 January 2012
Published as BJ Immediate Publication 3 January 2012, doi:10.1042/BJ20111308